EMG Control of a Bionic Knee Prosthesis: Exploiting Muscle Co-Contractions for Improved Locomotor Function

James A. Dawley and Kevin B. Fite
Department of Mechanical and Aeronautical Engineering
Clarkson University
Potsdam, NY USA

George D. Fulk
Department of Physical Therapy
Clarkson University
Potsdam, NY USA

***Abstract*— This paper presents the development and experimental evaluation of a volitional control architecture for a powered-knee transfemoral prosthesis that affords the amputee user with direct control of knee impedance using measured electromyogram (EMG) potentials of antagonist muscles in the residual limb. The control methodology incorporates a calibration procedure performed with each donning of the prosthesis that characterizes the co-contraction levels as the user performs volitional phantom-knee flexor and extensor contractions. The performance envelope for EMG control of impedance is then automatically shaped based on the flexor and extensor calibration datasets. The result is a control architecture that is optimized to the user's current co-contraction activity, providing performance robustness to variation in sensor placement or physiological changes in the residual-limb musculature. Experimental results with a single unilateral transfemoral amputee user demonstrate consistent and repeatable control performance for level walking at self-selected speed over a multi-week, multi-session period of evaluation.**

Keywords — lower-limb prosthetics, myoelectric control, powered prosthetics

I. INTRODUCTION

Recent advances in lower-limb prosthesis technology have resulted in the emergence of a number of active, externally-powered prosthetic knee systems for transfemoral amputees [1]-[8]. The net power generation capability provided by such devices holds the potential for enabling gait functions such as stair ascent, ramp ascent, standing from a seated position, and other functions where net-positive mechanical power is required to attain physiologically normal functionality [9]-[14]. The extent to which the bionic knee systems extend function beyond that of current microprocessor-controlled passive knees largely depends on the performance of the active-limb control system.

Approaches to control of energetically-active transfemoral prostheses can be segmented into two classes: those based on dynamic mechanical interaction between the user and limb and those based on surface electromyogram (EMG) measurements of muscle activity in the user's residual limb. Control based on mechanical interaction utilizes mechanical sensors integrated on the prosthetic limb and/or the contralateral limb combined with state-control methods [1]-[5] or echo-control methods [15]-[17] to modulate prosthetic-limb behavior within the gait cycle. Multiple locomotive functions are realized with the addition of pattern-recognition algorithms for inference of user intent based on the dynamic mechanical interaction between the prosthesis, user and environment. These control architectures have been shown to provide physiologically normal gait functionality for activities such as level walking and slope ascent, but do so without affording the amputee user with any means of volitionally modulating the mechanical output of the prosthesis.

In contrast, prosthetic-limb control based on surface EMG measurements provides a means for using muscle contractions in the amputee's residual limb to command or modulate the outputs of the prosthesis. Early efforts in EMG-based control of transfemoral prosthesis systems focused on using EMG commands for modulating the behavior of passive limb systems, including surface EMG control of knee locking/unlocking [18],[19] and knee power dissipation [20]. More recent work has focused on EMG modulation of control (where EMG measurements are used inputs to a pattern-recognition architecture for user-intent recognition) and direct EMG control (where the EMG commands directly control the mechanical output of the prosthetic knee). EMG modulation of control [21],[22] is often used within a finite-state control architecture, in which case the EMG potentials augment or replace the measured mechanical interactions as the inputs to the pattern-recognition algorithm that selects the appropriate predetermined prosthetic-limb state. Other work has focused on direct EMG control where residual-limb EMG has been shown effective for volitional knee control in nonweight-bearing motion tracking [23] and in locomotion [6],[24].

The work presented here builds upon the demonstrated potential of direct EMG control in weight-bearing locomotor function with the development of an impedance-based control methodology that is robust to time-variation in the amputee user's residual-limb EMG potentials. Rather than simply normalize each surface EMG measurement to its maximum voluntary contraction potential and otherwise assume the user has independent control of each instrumented muscle, the approach described here directly accounts for muscle co-contraction with each donning of the limb. The systematic procedure enables impedance-control parameters to be mapped

978-1-4673-6024-1/13/$31.00 ©2013 IEEE

directly to the user's co-contraction patterns, enabling the user to exploit the full performance capability of the prosthetic knee. Experimental results with a single unilateral transfemoral amputee subject indicate consistent session-to-session control performance in level-ground walking that is attained without the need for any inter-session adjustment of impedance control parameters in response to EMG variation. The variations are not eliminated, but the control architecture renders their effects transparent from the perspective of EMG control of prosthetic-knee impedance.

II. Subject Preparation and EMG Calibration

A single subject with unilateral transfemoral amputation was recruited for participation in this pilot study. The recruited subject was a 53 year-old, 83 kg male with a unilateral transfemoral amputation of the right leg due to traumatic injury. The participant was approximately four years post-amputation when this work commenced. The study was conducted with the approval of the Clarkson University IRB and the informed consent of the participant. It entailed identification and calibration of EMG control sites on the user's residual thigh, the development of a user-optimized control interface for direct EMG control of knee function, and experimental gait training and analysis.

The overall objective is EMG control of a bionic knee for locomotor and non-locomotor function. An integral component of this objective involves the identification and characterization of EMG activity of contractile muscles in the amputee's residual thigh that can be used for controlling the prosthetic knee. Bidirectional control of the bionic knee requires a minimum of two antagonist muscles over which the user exhibits volitional control of contraction. The participant was asked to perform volitional extension and flexion of his phantom knee while the residual thigh was manually palpated to locate active quadriceps and hamstring muscles. Once identified, a single antagonist muscle pair was instrumented with surface EMG electrodes (Otto Bock 13E202).

The subject was then asked to perform a periodic series of phantom-knee extensions at 25%, 50%, 75% and 100% of maximum extension intensity over a 60 s period while standing upright. The subject held each contraction level for 1-3 s followed by a relaxation period of 1-3 s. The surface EMG potentials of the instrumented quadriceps and hamstring muscles were recorded over this period at a sampling frequency of 1 kHz. The procedure was then repeated for phantom-knee flexion. This calibration routine provides a means by which to assess the maximum EMG potentials for each muscle while at the same time characterizing the degree to which the subject exhibits co-contraction of the antagonist pairs when executing each task.

Fig. 1 shows representative data recorded during calibrations recorded on two separate dates over a four-month period. The figures show quadriceps (u_e) and hamstring (u_f) EMG normalized to maximum voluntary contraction for phantom-knee extension (**blue**) and phantom-knee flexion (**red**). The data in Fig. 1(a) was recorded at the beginning of this study, and that of Fig. 1(b) was recorded over four months later. The figures highlight two of the challenges with respect to EMG control of a bionic knee. Firstly, note that the subject exhibits significant levels of co-contraction when performing the phantom-knee extension and flexion tasks. The EMG data of Fig. 1(a) shows 25-30% co-contraction of the antagonist muscle for each phantom-knee task. By comparison, the EMG data of Fig. 1(b) shows a comparable percentage of co-contraction for phantom-knee flexion, but improved isolation of quadriceps contractions during phantom-knee extensions. This co-contraction and its time-varying nature complicate the ability to obtain performance robustness with EMG control.

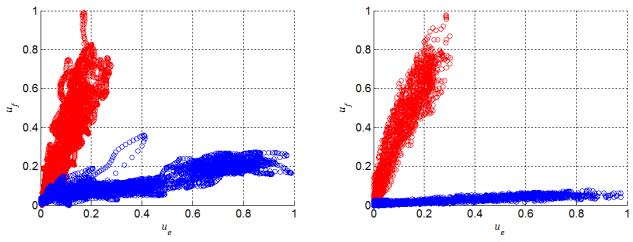

(a) (b)

Fig. 1. Normalized hamstring EMG (u_f) versus normalized quadriceps EMG (u_f) for phantom-knee extension (blue) and phantom-knee flexion (red) recorded at (a) the beginning and (b) end of a four-month period.

The authors' prior work in EMG control of a transfemoral prosthesis demonstrated two approaches to EMG control, both of which suffer from co-contraction of the antagonist muscle pairs. In the impedance control architecture of [6], co-contraction prevents the amputee user from exploiting the full performance envelope of the knee prosthesis. The proportional torque control architecture of [24] likewise suffers from the presence of co-contraction. Because the net torque output at the knee scales with the difference in EMG potentials between the two muscles, co-contraction results in cancelling flexor/extensor torques that prevent the full range of device torques from being achieved. To some extent, these problems are mitigated through tuning of control parameters. However, the time-varying nature of the co-contraction requires empirical tuning of control parameters with each donning of the prosthesis, thereby limiting the ability of each architecture to achieve robust and repeatable control performance.

The control architecture detailed in the Section III has thus been developed to exploit the natural co-contractions in the user's residual limb within a framework that is optimized to the user at each donning of the device. The objective is an EMG control interface that is robust to changes in residual-limb co-contraction and variation in electrode placement on the residual limb. The primary components of the control interface are an impedance control structure that directly leverages residual-limb co-contractions for prosthetic knee control and an initialization routine that directly maps the impedance control structure to the user's current state of co-contraction.

III. Impedance Manifold for EMG Control

The mechanical impedance of muscle has been shown to play a significant role in the dynamics of the musculo-skeletal system [18],[26]. An in-depth study of the role of antagonist muscle pairs has demonstrated that skeletal muscle modulates joint impedance as a function of the external load and link configuration [27]. Given the role of impedance in musculoskeletal mechanics and its fundamental relation to joint

actuation, modulation of limb impedance based on antagonist EMG activity offers a biomechanically appealing architecture for prosthetic knee control.

A. User-Optimized Impedance Manifold

The bounds of operation for EMG control of the bionic knee are established using the calibration routine described in Section II. With the surface EMG electrodes in place and the prosthesis donned, the user performs phantom-knee extension and flexion at various levels of contractile intensity using the described calibration procedure. The recorded EMG data characterizes the degree of co-contraction exhibited by the user and is used, as described below, to establish the bounds of the flexion/extension phase plane available for EMG control of prosthetic-knee impedance. The approach described below can be viewed as a variation of the methodology used for handling muscle co-contraction in volitional control of nonweight-bearing knee function [23]. However, the architecture outlined here differs fundamentally due to the fact that resulting flexion/extension phase plane is used as a means for the amputee user to independently control the impedance of the prosthetic knee joint and the rate-of-change of equilibrium point (in both magnitude and direction). This in turn will necessitate that the amputee user's EMG commands will vary continuously throughout the bounded region, rather than assumed to be constrained to one of the two boundaries.

Principle component analysis (PCA) is then applied separately to the phantom-knee flexion and extension data. The procedure involves subtraction of the mean, followed by computation of the eigenvalues and eigenvectors from the covariance matrix associated with each dataset. The principle components for such a two-dimensional dataset amount to a coordinate transformation that projects the data along its eigenvector directions. The boundaries of the impedance manifold are then found by taking the first principle component of each dataset and representing it in the original flexion/extension coordinate system.

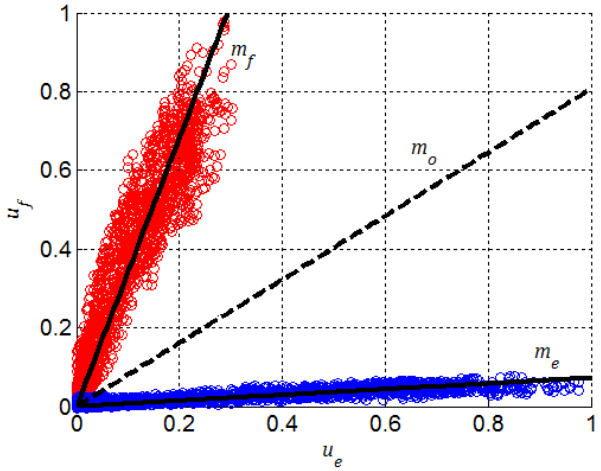

Fig. 2. Normalized hamstring EMG versus normalized quadriceps EMG for phantom-knee extension (blue) and phantom-knee flexion (red) with the flexion (m_f), extension (m_e), and transition (m_o) boundaries.

Fig. 2 shows an example of the results for the calibration dataset of Fig. 1(b). The boundaries as determined using PCA are represented by two lines of constant slope that pass through the origin. The slope of the flexion boundary is represented by m_f, and that of the extension boundary is represented by m_e. To further divide the operation envelope, a third line of constant slope m_o given by:

$$m_o = \tan\left(\frac{\tan^{-1} m_f + \tan^{-1} m_e}{2}\right) \tag{1}$$

is computed to bisect the envelope into two equal halves. This line represents the transition between flexion and extension. The region bounded by m_o and m_e represents the impedances biased to knee extension, whereas that bounded by m_o and m_f represents those impedances biased to knee flexion. Once the impedance space is segmented accordingly, the mapping between flexion/extension EMG and knee impedance is specified as described in the following section.

B. EMG Impedance Control

The impedance control architecture detailed below affords the amputee user with control of the stiffness and the rate-of-change of desired equilibrium point of the prosthetic knee. The commanded knee stiffness is given by:

$$K = K_{max}\sqrt{u_e^2 + u_f^2} \tag{2}$$

where K_{max} is a constant representing the maximum stiffness of the prosthetic knee, u_e is the normalized extensor EMG and u_f is the normalized flexor EMG. The magnitude of the user's total EMG activity is mapped to the stiffness exhibited by the prosthetic knee. The EMG-specified set point is then determined based on the distance the instantaneous EMG command lies away from the flexion/extension transition boundary. Rather than control desired position directly, the architecture is structured such that the user directly specifies the desired velocity of the knee joint.

The instantaneous EMG commands u_e and u_f are used to compute an instantaneous slope m, given by:

$$m = \frac{u_f}{u_e} \tag{3}$$

The rate-of-change of desired equilibrium point ω_d for the impedance of the prosthetic knee is then given by:

$$\omega_d = \begin{cases} \left(\frac{m - m_o}{m_f - m_o}\right)\omega_{max} & \text{if } m \geq m_o \\ \left(\frac{m - m_o}{m_o - m_e}\right)\omega_{max} & \text{if } m < m_o \end{cases} \tag{4}$$

where ω_{max} is the maximum allowable angular velocity of the prosthetic knee. If the instantaneous slope (m) exceeds the slope of flexion/extension transition, then the desired angular velocity of the knee equilibrium point is in the direction of flexion. Conversely, extensor command velocities result when the instantaneous slope is less than that of the flexion/extension boundary. The velocity command is zero at the flexion/extension transition, maximally positive at the flexion boundary, and maximally negative at the extension boundary. The desired equilibrium point θ_d is then obtained by integration of (4):

$$\theta_d = \int \omega_d \, dt \tag{5}$$

Note that for practical implementation, the output of this integral is saturated at the mechanical limits of the prosthetic knee. Using (1)-(5), the torque commanded to the prosthetic knee's servo controller is then given by:

$$\tau_d = K(\theta_d - \theta) - B\omega \tag{6}$$

where τ_d is the command torque; θ and ω are the angular position and angular velocity of the prosthetic knee; and B is a constant governing the viscous damping about the knee.

Fig. 3 provides a visualization of the impedance performance envelope for a given calibration dataset. The commanded stiffness is governed by the magnitude of the combined EMG signals. On the figure, lines of constant stiffness are denoted by the arcs of fixed radial distance from the origin. The rate-of-change of the desired equilibrium is specified by the arc angle between the line of instantaneous command (as determined by a line of slope m passing through the origin) and the flexion/extension transition line. In the context of polar coordinates, the radial and angular components govern the stiffness and rate-of-change of equilibrium, respectively, of the commanded prosthetic knee impedance.

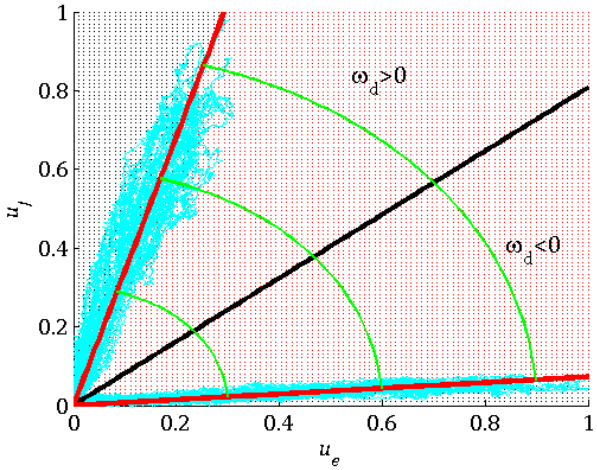

Fig. 3. Performance envelope for impedance control, as segmented by the flexion and extension boundaries (**red**) and the flexion/extension transition (**black**). The radial arcs (**green**) denote lines of constant knee stiffness.

IV. Experimental Results

Experimental evaluations were performed using a custom-designed transfemoral prosthesis prototype consisting of a single-degree-of-freedom motor-actuated knee joint, a composite energy-return ankle/foot (Otto Bock Journey 1E44), and a two-part diagnostic suction socket custom fit to the amputee participant by a certified prosthetist. Real-time control of the prototype is implemented using Matlab/Simulink and combines the impedance control architecture of Section III with low-level servo control of the torque output of the knee actuator. Additional details of the transfemoral prosthesis prototype can be found in [6] and [24].

Following development of the EMG control architecture, a training protocol and experimental gait studies were conducted to parameterize the gains for impedance control (i.e., K_{max}, B, and ω_{max}) and evaluate its performance and performance-robustness for locomotion of level ground. The impedance control gains were tuned over three two-hour sessions during which the participant performed nonweight-bearing tracking control tasks (both seated and standing), quiet double-support stance under full weight bearing, sit-stand transitions under full weight bearing, and treadmill walking with handrails for support. It should be noted that, having worked with the authors on previous EMG control developments, this subject had significant prior experience with EMG control of the transfemoral prosthesis. While the control architecture developed here differs significantly from those previously implemented, the user's past experience with the limb and EMG control interface enabled a relatively short progression from preliminary open-chain tracking tasks to demonstration of weight-bearing locomotor function. Table 1 shows the impedance control parameters resulting from the initial training sessions with the participant.

TABLE I
Impedance Control Parameters

Parameter	Units	Value
K_{max}	N·m/rad	50
B	N·m·s/rad	0.015
ω_{max}	rad/s	10

Fig. 4. Level walking with rolling-harness support.

Once the user demonstrated the ability to walk continuously on the treadmill without support of the handrails, open-floor walking tests were then conducted. The user was asked to walk back and forth along a 30 m segment of a flat tiled floor. The user performed the open-floor tests with a rolling harness system that provided support using a vertically-suspended shoulder harness. The harness provided no unweighting of the user but served to prevent fall or injury that might occur as a result of stumble or limb malfunction. A picture of the user walking with the rolling harness system is shown in Fig. 4. During the initial sessions, a clinical physical therapist walked behind the subject to help propel and navigate the rolling harness. However, once accustomed to prosthesis control in the open-floor setting, the subject was able to control the prosthesis while steering and propelling the rolling harness without the need for assistance from the physical therapist.

Data collected during the open-floor walking sessions included knee angle, actuator torque, pressure at the heel and

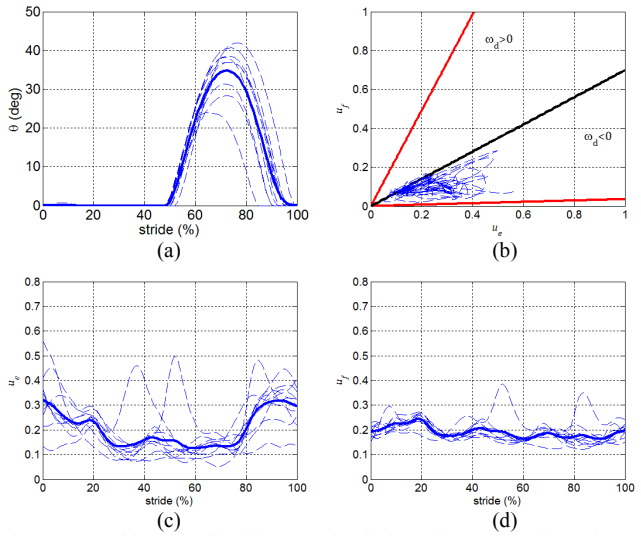

Fig. 5. (a) Stride-normalized knee angle, (b) impedance control envelope, (c) stride-normalized extensor EMG, and (d) stride-normalized flexor EMG for ten successive strides of open-floor walking at self-selected speed. The bold line in (a), (b), and (c) represents the ensemble average of each dataset. Data was collected during the first of four open-floor walking sessions.

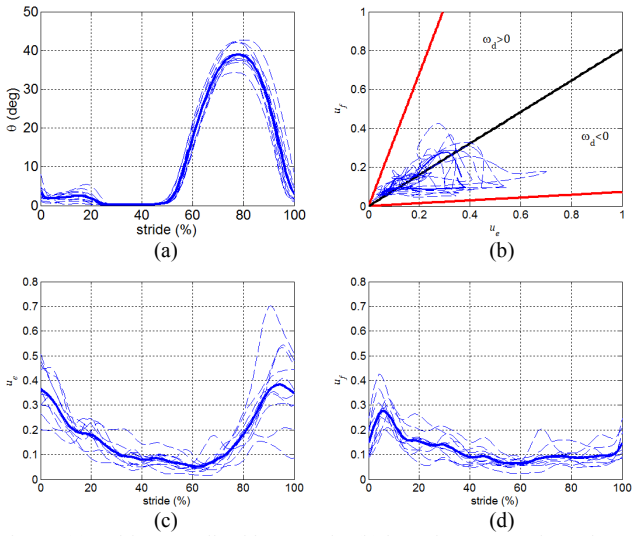

Fig. 6. (a) Stride-normalized knee angle, (b) impedance control envelope, (c) stride-normalized extensor EMG, and (d) stride-normalized flexor EMG for ten successive strides of open-floor walking at self-selected speed. The bold line in (a), (b), and (c) represents the ensemble average of each dataset. Data was collected during the fourth of four open-floor walking sessions.

ball of the prosthetic foot, and the EMG commands from the instrumented hamstring and quadriceps muscles. Each data stream is segmented into individual strides beginning with heel contact of the prosthesis and normalized to full stride (as measured from heel contact to heel contact of the prosthetic-side limb).

Fig. 5 shows the stride-normalized knee angle, impedance envelope, and EMG commands for ten successive strides of level walking at the user's self-selected speed. This data was collected during the first open-floor training session and thus represents early experimental results of the user's ability to walk with the limb using EMG impedance controller defined by (1)-(5). The stance phase of the walking gait ranges from 0-60% stride, and the swing phase encompasses the remainder. During stance, the user adopts a strategy that ensures the knee remains in full extension from the beginning of heel contact to just prior to the swing transition. This strategy is affected by the extensor EMG command (u_e) in combination with a hyper-extensor moment resulting from the user's loading of the limb anterior to the knee's center of rotation. During swing, the trajectories of the prosthetic knee exhibit significant variation in maximum flexion angle and it location within the gait cycle. This variation results from the significant EMG variation and can be attributed in part to the early point in the gait training cycle at which this data was collected. Since this data was collected during the first session of open-floor walking, the user was in all likelihood still developing an appropriate motor control strategy for walking with the EMG-controlled knee system.

As seen in the plot of the EMG commands within the impedance envelope, the user primarily stays within the extensor region of the envelope. The angular velocity command (ω_d) varies between zero and maximum extensor velocity, but never strays beyond the transition to flexor command velocities. The EMG-controlled stiffness of the prosthetic knee varies between zero and ~50% of the maximum allowable value (K_{max}). The points of maximum stiffness occur during late swing, as the user drives the limb into full extension prior to heel contact and during the onset of weight-bearing load in early- to mid-stance.

For comparison, Fig. 6 shows experimental results collected during the fourth of four training sessions of open-floor walking. The figure shows stride-normalized knee angle, impedance envelope, and EMG commands for ten successive strides of level walking at the user's self-selected speed. In contrast to the data collected during the first open-floor session, the variation in stride-normalized knee angle (Fig. 6(a)) is noticeably reduced. The knee exhibits consistent peak swing-phase angles of 40°, and these peaks occur consistently between 78-80% stride. In addition to the improvement in the swing-phase trajectories, the knee mechanics during stance are also improved relative to those of Fig. 5(a). The knee exhibits a moderate degree of stance flexion during early stance. This stance flexion serves to cushion the impact of heel contact and has the potential to lower the user's center of mass during single support (though this was not experimentally measured). The presence of stance flexion suggests that the user is beginning to exploit the impedance control architecture in a way conducive to realizing gait biomechanics similar to those of able-bodied individuals. The plot of the EMG commands within the impedance envelope (Fig. 6(b)) shows a broader use of the available performance space with consistent incursions into the flexor region of the angular velocity command. This increased usage of the available operation envelope is a contributor to the improved swing-phase consistency and the cushioning flexion at the onset of weight-bearing load. The magnitude of commanded knee stiffness does not appear to change significantly when comparing Figs. 5(b) and 6(b), but the user's improved trust in the EMG-controlled prosthesis allows better exploitation of the impedance-control parameter space.

It should be noted that once the impedance control parameters (i.e., K_{max}, B, and ω_{max}) were specified at the beginning of the experimental investigation of limb control, they remained unchanged over the course of the entire four-session sequence. In so doing, the amputee user was given sufficient time to acclimate to the impedance control architecture without the need for continual parameter adjustment in response to changes in EMG contraction signatures as a function of variation in EMG electrode placement or physiological changes in the residual limb. Both types of variation are adequately addressed with the calibration routine performed at each donning of the limb, freeing the amputee user to focus on improving volitional control within an architecture that is perceived as invariant from the perspective of EMG control of knee impedance.

V. Conclusion

The approach to EMG-based prosthesis control presented in this paper entails a systematic procedure for defining the impedance-control envelope that is mapped to the individual user's EMG contractions at each donning of the transfemoral prosthesis. This approach provides robustness to EMG measurement variation due to changes in electrode placement or variation in muscle co-contraction levels, which in turn contributes to the demonstrated consistency seen in the subject's ability to walk with the EMG-controlled prosthesis. Future efforts will focus on validation of the methodology with additional subjects and investigation of its extension to additional locomotive functions.

Acknowledgment

The authors would like to thank Donald W. Holmes of Northern Orthopedic Lab (Potsdam, NY) for his assistance in subject recruitment and the work he performed in fitting and alignment of the prosthesis to the participating subject.

References

[1] D. B. Popovic, R. Tomovic, L. Schwirtlich, and D. Tepavac, "Control aspects of above-knee prosthesis," International Journal of Man-Machine Studies, vol. 35, pp. 751-767, 1991.

[2] E. C. Martinez-Villalpando and H. Herr, H., "Agonist-antagonist active knee prosthesis: A preliminary study in level-ground walking," Journal of Rehabilitation Research & Development, vol. 46, no. 3, pp. 361-374, 2009.

[3] F. Sup, H. A. Varol, J. Mitchell, T. J. Withrow, and M. Goldfarb, "Preliminary Evaluations of a Self-Contained Anthropomorphic Transfemoral Prosthesis," IEEE/ASME Trans. on Mechatronics, vol. 14, no. 6, Dec. 2009.

[4] H. A. Varol, F. C. Sup, and M. Goldfarb, "Real-time multi-class intent recognition of a powered knee and ankle prosthesis", IEEE Trans. Biomed. Eng., vol. 57, no. 3, pp. 542-551, Mar. 2010.

[5] F. Sup, H. A. Varol, and M. Goldfarb, M. "Upslope walking with a powered knee and ankle prosthesis: initial results with an amputee subject," IEEE Trans. on Neural systems and Rehabilitation Engineering, vol. 19, no. 1, pp. 71-78, Feb. 2011.

[6] C. D. Hoover, G. D. Fulk, and K. B. Fite, "The design and initial experimental validation of an active myoelectric transfemoral prosthesis," ASME Journal of Medical Devices, vol. 6, no. 1, pp. 011005, Mar. 2012.

[7] C. Titley, "We have the technology," Engineering and Technology, vol. 4, no. 15, pp. 22-25, 2009.

[8] J. Z. Laferrier and R. Gailey, R., "Advances in lower-limb prosthetic technology," Physical Medicine and Rehabilitation Clinics of North America, vol. 21, no. 1, pp. 87-110, 2010.

[9] B. J. McFadyen and D. A. Winter, "An integrated biomechanical analysis of normal stair ascent and descent," Journal of Biomechanics, vol. 21, no. 9, pp. 733-744, 1988.

[10] R. Riener, M. Rabuffetti, and C. Frigo, "Joint powers in stair climbing at different slopes," Proc. IEEE International Conference on Engineering in Medicine and Biology, vol. 1, pp. 530, 1999.

[11] W. G. M. Janssen, H. B. J. Bussmann, and H. J. Stam, "Determinants of the sit-to-stand movement: a review", Physical Therapy, vol. 82, pp. 866-879, 2002.

[12] S. Nadeau, B. J. McFadyen, and F. Malouin, "Frontal and sagittal plane analyses of the stair climbing task in healthy adults aged over 40 years: what are the challenges compared to level walking?," Clinical Biomechanics, vol. 18, no. 10, pp. 950-959, 2003.

[13] A. N. Lay, C. J. Hass, T. R. Nichols, and R. J. Gregor, "The effects of sloped surfaces on locomotion: an electromyographic analysis," Journal of Biomechanics, vol. 40, no. 6, pp. 1276-1285, 2007.

[14] A. Vanezis and A. Lees, "A biomechanical analysis of good and poor performers of the vertical jump," Ergonomics, vol. 48, nos. 11-14, pp. 1594-1603, 2005.

[15] D. L. Grimes, "An active multi-mode above-knee prosthesis controller," Ph.D. Thesis, Department of Mechanical Engineering, MIT, Cambridge, MA, 1979.

[16] J. L. Stein and W. C. Flowers, "Stance phase control of above-knee prostheses: knee control versus SACH foot design," Journal of Biomechanics, vol. 20, no. 1, pp. 19-28, 1987.

[17] H. Vallery, R. Burgkart, C. Hartmann, J. Mitternacht, R. Riener, and M. Buss, "Complementary limb motion estimation for the control of active knee prostheses," Biomedizinische Technik / Biomedical Engineering, vol. 56, no. 1, pp. 45-51, 2011.

[18] G. W. Horn, "Electro-control: an EMG-controlled A/K prosthesis," Medical and Biological Engineering, vol. 10, no. 1, pp. 61-73, 1972.

[19] S. C. Saxena and P. Mukhopadhyay, "E.M.G. operated electronic artificial-leg controller", Medical and Biological Engineering and Computing, vol. 15, no. 5, 553-557, 1977.

[20] M. Donath, "Proportional EMG control for above knee prostheses," M. S. Thesis, Dept. Mech. Eng., MIT, Cambridge, MA, 1974.

[21] L. Peeraer, B. Aeyels, and G. Van der Perre, "Development of EMG-Based mode and intent recognition algorithms for a computer-controlled above-knee prosthesis," Journal of Biomedical Engineering, vol. 12, no. 3, pp. 178-182, May 1990.

[22] H. Huang, T. A. Kuiken, and R. D. Lipschutz, "A strategy for identifying locomotion modes using surface electromyography," IEEE Trans. Biomed. Eng., vol. 56, no. 1, pp. 65-73, Jan. 2009.

[23] K. H. Ha, H. A. Varol, and M. Goldfarb, "Volitional control of a prosthetic knee using surface electromyography," IEEE Trans. Biomed. Eng., vol. 58, no. 1, pp. 144-151, Jan. 2011.

[24] C. D. Hoover, G. D. Fulk, and K. B. Fite, "Stair ascent with a powered transfemoral prosthesis under direct myoelectric control," IEEE/ASME Transactions on Mechatronics, in press.

[25] E. Bizzi, A. Polit, and P. Morasso, "Mechanisms underlying achievement of final head position," Journal of Neurophysiology, vol. 39, no. 2, pp. 435-444, 1976.

[26] E. Bizzi, P. Dev, P. Morasso, and A. Polit, "Effect of load disturbances during centrally initiated movements," Journal of Neurophysiology, vol. 41, no. 3, pp. 542-556, 1978.

[27] N. Hogan, "Adaptive control of mechanical impedance by coactivation of antagonist muscles," IEEE Trans. on Automatic Control, vol. 29, no. 8, pp. 681-690, 1984.